Composite Science and Technology, (2008) submitted

Characterization of Brazed Joints of C-C Composite to Cu-clad-Molybdenum

M. Singh[1] and R. Asthana[2*]

[1]Ohio Aerospace Institute,
MS 106-5, Ceramics Branch
NASA Glenn Research Center
Cleveland, OH 44135

[2]Department of Engineering and Technology
University of Wisconsin-Stout
Menomonie, WI 54751

Abstract

Carbon-carbon composites with either pitch+CVI matrix or resin-derived matrix were joined to copper-clad molybdenum using two active braze alloys, Cusil-ABA (1.75% Ti) and Ticusil (4.5% Ti). The brazed joints revealed good interfacial bonding, preferential precipitation of Ti at the composite/braze interface, and a tendency toward de-lamination in resin-derived C-C composite due to its low inter-laminar shear strength. Extensive braze penetration of the inter-fiber channels in the pitch+CVI C-C composites was observed. The relatively low brazing temperatures (<950°C) precluded melting of the clad layer and restricted the redistribution of alloying elements but led to metallurgically sound composite joints. The Knoop microhardness (HK) distribution across the joint interfaces revealed sharp gradients at the Cu-clad-Mo/braze interface and higher hardness in Ticusil (~85-250 HK) than in Cusil-ABA (~50-150 HK). These C-C/Cu-clad-Mo joints with relatively low thermal resistance may be promising for thermal management applications.

Keywords: Scanning electron microscopy (D), Welding/Joining (E), Metals (A), Hardness testing (D), Carbon-carbon composite.

[*] Corresponding author: R. Asthana, email: asthanar@uwstout.edu, Fax: (216)433-5544

1. Introduction

A number of thermal management applications utilize copper-clad-molybdenum and copper-clad-invar because of their tailorable thermal conductivity and low thermal expansion properties. However, the high density of these materials (e.g., 9,700 and 8,450 $kg.m^{-3}$ for Cu-clad-Mo and Cu-clad-invar, respectively) has limited their use in lightweight heat rejection systems. In order to reduce the weight without sacrificing the thermal conductivity and thermal expansion benefits, copper-clad-molybdenum has been joined to graphite [1] and more recently, to C-C composites [2]. Carbon-carbon composites containing high-conductivity carbon fibers provide excellent heat dissipation and low expansion properties at considerably reduced weight. For example, the axial thermal conductivity of high-modulus (HM) and ultra-high modulus (UHM) carbon fibers are ~120-300 W/m.K and ~500-1100 W/m.K, respectively [3]. The thermal conductivity of Cu-clad Mo varies with the clad layer thickness and is in the range 138-235 W/m.K for 0 to 30% Cu layer thickness per side of Mo substrate [4]; the conductivity at 30% clad layer thickness is comparable to the conductivity of lightweight aluminum (237 W/m.K, density: 2,700 $kg.m^{-3}$), a good thermal conductor, but slightly inferior to the thermal conductivity of the heavier copper (391 W/m.K) with a density of 8,940 $kg.m^{-3}$. Acting in combination at a joint, Cu-clad Mo and C-C composite can provide excellent heat dissipation capability at reduced weight compared to the heavier Cu-clad Mo acting in isolation. The coefficient of thermal expansion (CTE) of Cu-clad Mo varies from ~$5.6x10^{-6}$/K to $11.6x10^{-6}$/K for 0 to 30% clad layer thickness [4] whereas the CTE of C-C composites is ~$2.0\text{-}4.0\times10^{-6}$/K over the temperature range 20-2500°C [3]. Thus, the CTE mismatch between C-C and Cu-clad Mo can be designed to minimize residual stresses during joining and service while still maintaining good thermal conductivity for use in heat rejection systems.

In a recent study [2], we had brazed resin-derived C-C composites containing T300 C fibers to Cu-clad-Mo using four active brazes: Cu-ABA, Ticuni, Ticusil and Cusin-1 ABA. In the present work, we report the brazing and joint characterization of 3D C-C composites having pitch+CVI carbon matrices to Cu-clad-Mo for heat rejection applications using two Ti-containing Ag-Cu active braze alloys (Ticusil and Cusil-ABA). The alloys Ticusil and Cusil-ABA have thermal conductivity either higher than or comparable to the conductivity of braze alloys used in our earlier study [2]. The thermal conductivity of Cusil-ABA (180 W/m.K) is better than that of Cu-ABA (38 W/m.K) and Cusin-1 ABA (170 W/m.K) used in our earlier work. In addition, the ductility of Cusil-ABA (42%) is better than the ductility of Cusin-1 ABA (22%) and comparable to Cu-ABA (42%). Both

Cusil-ABA and Ticusil are Ti-containing active braze alloys (ABA) that are expected to wet the carbon. In recent publications [5-8], we had reported on the use of these and similar brazes to join C-C, monolithic ceramics, and ceramic-matrix composites to various other substrates.

Some comments are in order to justify the use of 3D C-C composites with CVD carbon matrices in place of resin-derived matrices used in our earlier work [2]. First, 3D fiber structure overcomes the problems of poor mechanical properties perpendicular to 1D and 2D laminate planes. Second, complex 3D constructions are possible, including those with yarns oriented on polar coordinates in the radial, axial and circumferential directions (to accommodate hoop stresses in tubular components). Third, the use of CVI to deposit the matrix carbon offers some distinct advantages. In CVI, carbon is directly deposited onto the fiber surface whereas with liquid resin precursors, the carbon is produced in the void between the fibers after a thermal treatment. The resulting volumetric changes lead to porosity and shrinkage cracks in resin-derived carbon matrix when compared to CVI carbon matrix. In addition, because CVI deposits carbon mainly on the fiber surface, it is better suited than precursor-based methods for the production of thin sections which may be needed in thermal management applications. Finally, the thermal conductivity of CVI C-C composites is either comparable to or better than the thermal conductivity of resin-derived composites making the former more suitable for thermal management applications. For example, the thermal conductivity of CVI C-C at about 300°C is ~100-400 W/m.K whereas the conductivity of C-C with pitch- and resin-derived matrices is ~60-140 W/m.K at 300°C [3]. In CVI composites, the conductivity and expansion are determined by the preferred orientation, and their values can approach single crystal graphite values (although these properties depend also on a number of other factors such as the type of matrix carbon, matrix structure - smooth, rough, isotropic, laminar-, fiber architecture, and residual porosity).

In the present study, we investigated the vacuum brazing of CVI 3D C-C composites to Cu-clad-Mo using two Ag-Cu brazes: Cusil-ABA (1.75% Ti) and Ticusil (4.5% Ti). The presence of Cu as a cladding on Mo and as an alloying additive in the braze alloys is expected to promote the metallurgical continuity across the joint while providing interfacial ductility to mitigate the CTE mismatch induced stresses. A limited number of runs were made with resin-derived C-C composites to generate comparative base-line data on joining response. The brazed joints were characterized using optical microscopy, field emission scanning electron microscopy (FESEM), energy dispersive spectrometry (EDS), and by microhardness measurements.

2. Experimental Procedure

The 3-D carbon-carbon composites used in this study were made from P120 carbon fiber and an amorphous CVI carbon matrix, and were obtained from B.F. Goodrich Corp., Santa Fe, CA. These composite substrates were sectioned along two orthogonal directions to expose fiber plies with different fiber arrangements; thus, two sets of composite samples were used for joining: those with oriented fibers at the exposed C-C surface and those with random (non-oriented) fibers at the exposed surface. Some joints were made of carbon-carbon composites with T-300 fibers and resin-derived matrix, which were obtained from Carbon-Carbon Advanced Technology (C-CAT Composites) Inc., Fort Worth, TX. Copper-clad Molybdenum (Cu-Mo-Cu) plates from H.C. Starck, Inc., Newton, MA, were used as the metal substrate. The Cu-to-Mo-to-Cu layer thickness ratio was 13%-74%-13%. The Cu-Mo-Cu laminate was manufactured by rolling a Mo core sandwiched between two Cu layers. The material combines the high conductivity of Cu with the low coefficient of thermal expansion (CTE) of Mo; the CTE of the clad material is tailored by changing the clad ratio of Cu-Mo-Cu. The commercial brazes, Cusil-ABA and Ticusil, were in powder form and obtained from Morgan Advanced Ceramics, Hayward, CA. The compositions, liquidus and solidus temperatures, and selected physical and mechanical properties of the braze alloys are given in Table I.

The composite panels and Cu-clad Mo plates were sliced into 2.54 cm x 1.25 cm x 0.25 cm pieces. All materials were ultrasonically cleaned in acetone for 15 min. prior to brazing. The braze powders were mixed with glycerin to create a thick paste with dough-like consistency, and applied manually to the C-C surface using a spatula. The Cu-clad-Mo plate was laid over the braze layer and a load of 0.30-0.4 N was applied to the assembly. The assembly was placed in a vacuum furnace with the composite on top and Cu-clad-Mo at the bottom. The samples were heated to the brazing temperature (typically 15-20 °C above the braze liquidus) under vacuum (~10^{-6} torr), isothermally held for 5 min. at the brazing temperature, then slowly cooled (~5ºC per min.) to 400ºC followed by furnace cooling to room temperature.

The brazed joints were mounted in epoxy, ground and polished, and examined using optical microscopy, and Field Emission Scanning Electron Microscopy (FESEM) (model: Hitachi 4700) coupled with energy dispersive x-ray spectroscopy (EDS). Microhardness scans were made with a Knoop indenter across the joint interfaces on a Struers Duramin-A300 machine under a load of 200

g and loading time of 10 s. To check the reproducibility of the hardness profiles, multiple (typically 4 to 6) scans were made across each joint.

3. Results and Discussion

3.1 Braze Spreading and Infiltration

Prior to actual joining, a preliminary screening of braze spreading behavior was undertaken on the two types of C-C composite substrates: P120 C fiber in a CVI-carbon matrix, and T300 fiber in a resin-derived carbon matrix. This was done mainly because wettability data on C-C composite substrates containing different types of carbon fibers and carbon matrices are scarce although there is considerable data in the literature on wettability of Ag-Cu-Ti alloys on monolithic carbon substrates (e.g., vitreous, pyrolytic, diamond). Only a qualitative assessment of the spreading behavior was attempted, and the actual measurements of contact angles were not done. Figure 1 shows the photographs at the conclusion of the solidification of Cusil-ABA and Ticusil braze droplets equilibrated on the substrates at 813ºC and 915 ºC, respectively, after 5 min. contact with the C-C substrates. Both braze alloys displayed good spreading on the C-C substrates, with Ticusil exhibiting a somewhat better surface coverage than Cusil-ABA. This is believed to be due to the higher Ti content of Ticusil (4.5%Ti) than Cusil-ABA (1.75%Ti), which should enhance the reactive wetting. In fact, both pure Ag and Cu make large contact angles, θ, (θ~137°-140°) [9] on carbon, and both metals have large surface tension, σ_{lv} (σ_{lv}=925 N/m at 960°C for Ag, and σ_{lv}=1330 N/m at 1086°C for Cu [10]) which indicates that these metals in a pure state do not wet carbon. Titanium additions to Ag and Cu markedly and rapidly decrease the θ [9,11-13]; for example, θ approaches 0° in 5 min. at 1350°K for Cu containing 9wt%Ti in contact with vitreous C [12] and θ approaches a value of 10° at 1373°K for Cu containing 17.5wt%Ti in contact with porous graphite. Silver additions to Cu-Ti alloys are known to reduce the surface tension and significantly increase the Ti activity coefficient which aids chemical interaction of carbon with titanium and forms the wettable compound titanium carbide. In the case of silver, just 1wt% Ti in Ag at 1273°K decreases the θ on graphite to 7°. Thus, Ti renders non-wettable pure metals Ag and Cu nearly completely wettable. As a result, spreading and infiltration can continue because the reaction formed carbide is wettable by the molten AgCuTi braze alloys (θ=70° at 1273°K for Ag-28Cu-2Ti melt on TiC [9]).

The microstructures of the composite/braze interface and braze/Cu-clad-Mo interface in Cu clad Mo/C-C composite joints are shown in Fig. 2. Both Cusil-ABA and Ticusil have infiltrated the inter-fiber regions in the 3-D C-C composite. There was no effect of fiber ply orientation at the

mating surface on the extent of infiltration. Large-scale counter-gravitational infiltration (with composite on top, and Cu-clad-Mo at the bottom) has occurred during the short brazing time of 5 min. because of good wettability ($\theta < 90^{o}$). Low-magnification optical views suggest that infiltration distance is on the order of several hundred micrometers within the C-C composites. This is significant because the carbide forming reactions did not choke the metal flow or limit the extent of braze infiltration. The TiC reaction layer that forms via the reaction Ti + C → TiC is known to be discontinuous with a non-homogenous structure [14]; this permits extensive infiltration of porous carbon by the melt even in a short time interval of 5 min. This behavior is in contrast to the behavior exhibited by Cu-Cr melts on porous carbon where a dense chromium carbide layer forms and chokes the metal flow, thereby severely limiting the infiltration in spite of excellent wettability [14]. Our observations of extensive infiltration of Ti-bearing Ag-Cu braze alloys in the C-C composites are consistent with the sessile-drop wettability test results of Sobczak et al [15] on Cu-Ti/carbon system. These authors noted that the sessile drop volume continuously decreased due to the reactive infiltration of open porosity in graphite; in fact, sessile drops of high Ti content (e.g., Cu-28Ti) rapidly and completely disappeared into the graphite substrate [15].

3.2 Joint Microstructure and Composition

Figures 2 through 6 show the joint microstructure of C-C composite with Cu-clad-Mo. All joints display intimate physical contact at the composite/Cu-clad-Mo interface. The contact region and the braze region are free of common structural imperfections such as interfacial microvoids, shrinkage cavities, and micro-cracks. The dissolution of the Cu cladding from the Mo surface has enriched the braze with Cu, and led to the precipitation of a copper-rich phase at the joint- and within the inter-fiber regions (Fig. 2). The fiber ply orientation at the joint interface had no influence either on the infiltration distance or the microstructure of the joint.

The EDS elemental compositions at the composite/braze and braze/Cu-clad-Mo interfaces are given in in Tables 2 through 9. The distribution of the other major alloying elements across the joint region in different samples is also given in these tables. Only relative atomic percentages among the alloying elements are provided. A higher titanium concentration is observed at the composite/braze interface (e.g., point 2 in Fig. 3b & 4b) than in the nearby regions of the joints. The preferential segregation of Ti at the composite/braze interface is consistent with the high chemical affinity of Ti toward C, which promotes braze spreading and bonding. Improvement in spreading is promoted by the formation of the TiC (and wettable sub-stoichiometric carbides such as $TiC_{0.95}$,

$TiC_{0.91}$, $TiC_{0.80}$, $TiC_{0.70}$, $TiC_{0.60}$ and $TiC_{0.48}$). The Gibb's free energy change for TiC formation via Ti+C→ TiC at a brazing temperature of 850° C is -171.18 kJ, which suggests that TiC formation is possible. The Ag-Cu-Ti ternary diagram shows that at the brazing temperatures used (835 and 920°C), alloys with Ti>5at% yield a Ti-impoverished liquid phase and a Ti-rich liquid phase. It is conceivable that this Ti-rich liquid reacts with the carbon to form the carbides and a metallurgical bond. Besides carbide formation, Ti could react with minute amounts of residual oxygen in the furnace atmosphere (or in the surface scale on C-clad-Mo) leading to oxy-carbides and oxides such as the wettability-enhancing, metal-like compound TiO, which is known to form an interfacial layer on carbon.

The interfacial concentrations of Ti are larger in joints made with Cusil-ABA (point 2, Tables 2 & 4) than in joints made using Ticusil (point 4, Table 6). The EDS analyses show that diffusion of Ag, Mo and Ti in the composite matrix is negligible. The braze matrix exhibits a two-phase eutectic structure with Ag-rich light-grey areas (point 3, Fig. 3) and Cu-rich dark areas (point 4, Fig. 3). In the Ag-Cu-Ti system, intermetallics such as AgTi, Ti_2Cu_3, and $TiCu_2$ may also form.

The Cusil-ABA/Cu-clad-Mo interface (Fig. 3c) displays evidence of good wetting and somewhat diffuse interface character. The light-grey (Ag-rich) and dark (Cu-rich) eutectic micro-constituents are distributed within the braze region. The Cu cladding at the braze/Cu-clad-Mo interface appears to be intact because the joining temperature (830ºC) is below the melting point of Cu (1086ºC); however, some chemical dissolution has probably occurred at the Cu-cladding/braze interface. Very small quantities of Mo, Ag and Ti have diffused in the Cu cladding (Tables 3 & 5) and these elements did not lower the liquidus temperature sufficiently to cause melting of the cladding; this is evident from a lack of any conceivable sign of solidification microstructure in the clad layer.

Small amounts of Ag and Cu from braze are detected within the C-C composite region (point 1, Fig. 4b) but no measurable quantity of Mo is noted. The C-C/Cusil-ABA interface is rich in titanium and the Ti concentration decreases rather systematically with increasing distance from the interface (9.2 atom%, 4.2 atom% and 1.8 atom% at points 2, 4 and 5, respectively, in Fig. 4b).

In C-C/Cu-clad-Mo joints made using Ticusil (Fig. 5), a small amount of Cu is detected within the composite region (points 5 and 6, Fig. 5b). The normal two-phase eutectic structure with a characteristic acicular morphology (Fig. 5b & c) is observed within the braze region. Some carbon has dissolved in the molten braze, possibly because of the higher brazing temperature (915ºC) of Ticusil which led to C diffusion in the eutectic micro-constituents (points 1 and 2, Fig. 5b). In addition, carbon is detected within the Cu-clad-Mo region (points 3-6, Fig. 5c). Finally, as stated in

a preceding paragraph, oxygen (from the copper oxide scale on Cu-clad-Mo) could also be playing a role. Upon contact with the molten braze, the scale will dissociate and dissolve, yielding an oxygen-rich braze layer. As a result, besides carbides, oxides such as TiO and TiO_2 may also form at the C-C/metal joint because stable oxides of Ti can form at very low oxygen partial pressures.

Figure 6 shows joint interfaces between resin-derived C-C composite (C-CAT Composites) and Cu-clad-Mo made using Ticusil. Microstructurally sound joint interfaces have formed but there is some cracking within the C-C composite (Fig. 6a) presumably due to the low inter-laminar shear strength of C-C composites. Ag- and Cu-rich phases have formed in the braze matrix with the Ag-rich phase preferentially precipitating onto both C-C surface (point 2, Fig. 6b) and Cu-clad-Mo surface (point 2, Fig. 6c). A small amount of Cu is detected within the composite (point 4, Fig. 6b). Both C-C/Ticusil and Ticusil/Cu-Mo interfaces in the joint region appear to be defect-free.

In summary, whereas extensive chemical interactions did not occur and optically visible interfacial reaction layers did not form at the C-C/CuAgTi interfaces in joints, some redistribution of chemical species (e.g., carbon dissolution in braze) seems to have occurred. Large titanium concentrations occurred at the C-C/braze interface which indicated that surface modification, presumably a carbide-forming reaction, had promoted the wetting and bonding.

3.3 Microhardness

The distribution of Knoop microhardness (HK) across the C-C composite/Cu-clad-Mo joints made using Cusil-ABA and Ticusil is shown in Fig. 7. Because microhardness tests outcomes are sensitive to the actual measurement path and the distribution of metallurgical phases (e.g., carbides, brittle intermetallics etc), multiple hardness scans across each joint were made to confirm the reproducibility and consistency of the data. The hardness profiles of Fig. 7 show that fiber ply orientation did not affect the HK distribution either within the Cu-clad Mo region or within the braze region. Additionally, there was no effect of the composite type (CVI versus resin-derived) on the HK values recorded within the braze region. The hardness of the molybdenum substrate is ~200-330 HK. The hardness of the braze region depends on braze type; Ticusil (Fig. 7a,b & d) exhibits a higher hardness (~85-200 HK) than Cusil-ABA (~50-150 HK). This is consistent with the somewhat greater hardening expected in Ticusil (4.5%Ti) than in Cusil-ABA (1.75%Ti), and with the somewhat larger residual stresses expected with Ticusil because of its higher liquidus temperature (T_L ~ 920°C) than with Cusil-ABA (T_L ~ 815°C). Additionally, residual stresses due to

mismatch of coefficients of thermal expansion (CTE) can also rather significantly influence the hardness values.

3.4 Residual Stress at the Joint: Upon cooling the brazed joint from an elevated temperature, tensile and shear stresses are induced that weaken the joint and may cause failure. Large residual stresses arising from a mismatch of CTE can appreciably lower the fracture strength of the ceramic. For the C-C/Cu-clad-Mo joints, the CTE (α) of Cu-clad Mo is ~5.6 – 11.6x10^{-6}/K [4] and the CTE of C-C composites is ~2.0-4.0×10^{-6}/K over 20-2500°C [3]. The CTE mismatch ($\Delta\alpha$) between C-C and Cu-clad Mo is, therefore, moderate, and the thermoelastic stresses that develop during brazing and subsequent service may be accommodated without causing joint failure. The CTE of the metallic braze alloys used in our study is very large (18.5×10^{-6}/K, Table 1) which will give rise to large elastic thermal strain, $\Delta\alpha\Delta T$ ($\Delta\alpha$: CTE mismatch, ΔT: temperature interval) at the braze/composite and braze/Cu-clad Mo interfaces. To understand the effect of residual stresses on the integrity of the joint, simultaneous effects of the plasticity of the braze interlayer and the CTE mismatch between the three materials responding to temperature excursions must be considered.

Analytical and numerical models [16-21] have been developed to determine the residual stresses at joints between dissimilar materials. For example, Eager and coworkers [16-18] have developed numerical and analytical models of residual stress relief by metal interlayers taking into account the CTE mismatch and interlayer plasticity. Their models permit estimation of the strain energy in the ceramic for well-bonded ceramic-metal joints. For a small CTE mismatch between the ceramic (C) and the metal substrate (M), but with a large CTE mismatch between the ductile interlayer (I) and the base materials, which is the case with our joints (even though C-C is not a ceramic), the elastic strain energy, U_{eC}, in the ceramic can be approximated by [17]

$$U_{eC} = \frac{\sigma^2{}_{YI}.\Phi.r^3}{E_C}(0.26\Pi_I + 0.54) \qquad \text{.....[1]}$$

where

$$\Phi = 1 - (\frac{\alpha_M - \alpha_I}{\alpha_C - \alpha_I})^m \qquad \text{.....[2]}$$

and

$$\Pi_I = \frac{(\alpha_M - \alpha_C)\Delta T E_I}{\sigma_{YI}} \qquad \text{.....[3]}$$

Here, σ_{YI} is the yield strength of the interlayer, r is the radial distance from the center of the joint, E_C and E_I are the elastic modulus of the ceramic and the interlayer, respectively, ΔT is the temperature change, and α is the CTE of the subscripted phases (M, C, and I). The exponent m=1 for $\alpha_I > (\alpha_M + \alpha_C)/2$, and m=–1 for $\alpha_I < (\alpha_M + \alpha_C)/2$. Eager et al noted these equations to be accurate to 1% relative to their rigorous finite element calculations.

The parameters Π_I and Φ in the above equations are dimensionless quantities. The parameter Π_I is the ratio of the thermal residual strain at the interface to the yield strain of the braze interlayer; the smaller Π_I is, the larger the portion of the interface that remains elastic. The parameter Φ specifies the relative difference in CTE's between the ceramic (C), braze interlayer (I), and metal substrate (M), and it quantifies the uniformity and symmetry of the residual stress distribution in the interlayer. As Φ approaches zero, the stress distribution in the interlayer becomes more symmetric, which in turn, causes a larger volume of the braze to deform plastically and lower the strain energy in the ceramic, thus reducing the probability of failure from residual stresses.

The strain energy in the C-C/Cu-clad-Mo joints with Ticusil and Cusil-ABA interlayers was computed using the following property data: $\alpha_I = 18.5\times10^{-6}$/K (Table 1), $\alpha_C = 3\times10^{-6}$/K (average CTE for C-C composite) [22], m = 1 for C-C/Ticusil/Cu-clad-Mo joint, E_C = 70 GPa [3], E_I = 85 GPa (Table 1), ΔT = 887ºC, and σ_{YI} = 292 MPa (Table 1). The CTE values of Cu-clad-Mo (α_M) were obtained as a function of clad layer thickness from the data presented in ref. [4]; these values vary in the range 5.6×10^{-6}/K to 11.6×10^{-6}/K for clad layer thickness of 0% to 40% [4]. Using the above properties data, the elastic strain energy, $U_{eC} = 152.98 \times10^3.r^3$ where r is the radial distance in meters. The configuration analyzed by Eager et al [17] is a cylindrical disc-shaped joint whereas out joints are rectangular in cross-section (2.54 cm × 1.25 cm). As a first approximation, we take an effective radius of our joints to be the minimum distance to the edge of our samples (0.625 cm). This yields the elastic strain energy in the C-C/Cu-clad-Mo joints in the range 31-180 mJ, which is roughly of the same order as the U_{eC} (~ 0.5-80 mJ) of a number of ceramic-metal joints [16-18]. Considering the fact that the model strictly applies to a cylindrical (disc)-shaped joint configuration and monolithic ceramics rather than anisotropic (non-ceramic) materials such as C-C composites, and the fact that chemical interactions and solute segregation will irrevocably and unpredictably modulate the interphase properties, the calculated strain energy is probably representative of the real situation. The fact that there is a relatively large amount of porosity in the virgin 3D C-C composite and that some of the open porosity near the joint interface gets impregnated with the ductile braze

during joint formation suggests that some strain relief will be possible within the composite. The absence of fracture in our CVI C-C composite joints is consistent with this observation.

3.5 Thermal Conduction in Brazed Joints: For heat rejection applications, the thermal resistance of the joined assembly relative to the resistance offered by the individual constituents is important. For one-dimensional steady-state heat conduction, the joined materials form a series thermal circuit with an effective thermal resistance, R_{eff}, given from $R_{eff} = \Sigma(\Delta x_i/K_i)$, where Δx_i and K_i represent the thickness and the thermal conductivity, respectively, of the i^{th} layer. For the joints created in this work, $\Delta x_{C\text{-}C} = \Delta x_{Cu\text{-}Mo} = 0.25\times10^{-2}$ m, $\Delta x_{Braze} \sim 100\times10^{-6}$ m, $K_{Ticusil} = 219$ W/m-K (Table 1), and $K_{Cusil\text{-}ABA} = 180$ W/m-K (Table 1). The value of the thermal conductivity of Cu-clad-Mo, $K_{Cu\text{-}Mo}$, varies with the clad layer thickness, and is taken from ref. [4]; $K_{Cu\text{-}Mo}$ varies from 138 W/m-K to 235 W/m-K for 0 to 30% clad layer thickness [4]. For C-C composites, $K_{C\text{-}C}$ is anisotropic and varies considerably; for example, for 2D and 3D composites, $K_{C\text{-}C} = 60$ and 190 W/m-K [3] perpendicular and parallel to the carbon cloth at 500K, and for 1D composites, $K_{C\text{-}C} = 300$ W/m-K at 500K [3]. Taking the average $K_{C\text{-}C}$ to be 125 W/m-K for 2D and 3D composites, the effective thermal resistance of our joint assemblies can be computed for a range of clad layer thicknesses. The results shown in Fig. 8 indicate that R_{eff} varies in the range 31.5 to 38.5×10^{-6} m^2.K/W, and that there is insignificant (<1%) difference between Ticusil and Cusil-ABA. Because the difference in the R_{eff} of the joints with the two brazes is insignificant, there may be considerable flexibility in selecting brazes to satisfy other criteria such as ductility and wetting characteristics without impairing the thermal conductivity and weight advantages of the joined materials.

Figure 8 also compares the R_{eff} values of the joints to the R_{eff} values of C-C and Cu-clad-Mo substrates of the same total thickness (5.1×10^{-3} m) as the joined materials; the thermal resistance of the C-C block is about 40.8×10^{-6} m^2.K/W and that of a Cu-clad-Mo substrate is 22.8×10^{-6} m^2.K/W. The decrease in the thermal conductivity of our joints (with the Cu-clad-Mo substrate having a Cu:Mo:Cu thickness ratio of 13%:74%:13%) relative to an isolated Cu-clad-Mo substrate is compensated by a 39% decrease in the weight of the assembly. The Rule-of-Mixtures (ROM) density (ρ) of our joints is ~5,919 kg.m^{-3} (with $\rho_{C\text{-}C} = 1{,}900$ kg.m^{-3}) compared to a density of 9,937 kg.m^{-3} for Cu-clad-Mo alone (ignoring the thin braze interlayer does not introduce any sensible error in the density calculations).

Similar calculations for the thermal resistance of the joints can be made for 1-D C-C composite joined to Cu-clad-Mo. For 1D C-C composites ($K_{C\text{-}C} = 300$ W/m-K), the effective thermal

resistance of the assembly will be 19.9×10^{-6} m^2.K/W, and for a C-C substrate of the same total thickness as the joined assembly (5.1×10^{-3} m), the thermal resistance will be 17.0×10^{-6} m^2.K/W, which is only about 18% less than the effective resistance of the assembly. These simplified thermal considerations illustrate the potential benefits of joining C-C to Cu-clad-Mo to create light-weight heat rejection systems.

4. Conclusions

Carbon-carbon composites with either pitch+CVI matrix or resin-derived matrix were joined to copper-clad molybdenum using two Ti-containing active braze alloys (Cusil-ABA and Ticusil). Large-scale braze penetration of the inter-fiber spaces in the CVI C-C composites was observed. The SEM and EDS examination of brazed joints revealed good interfacial bonding in all C-C/Cu-clad-Mo joints, some diffusion and redistribution of alloying elements, and preferential segregation of Ti at the composite/braze interface. The distribution of microhardness across the joints was reproducible, consistent with the Ti content in the braze, and indicated sharp gradients at the Cu-clad-Mo/braze interface. The metallurgically sound composite joints produced in this work, and the projected benefits of reduced thermal stress and thermal resistance, suggest that C-C composite/Cu-clad-Mo joints may be attractive for potential applications in thermal management systems.

Acknowledgement: Technical assistance of Tarah P. Shpargel is thankfully acknowledged. R. Asthana acknowledges the research support received from the NASA Glenn Research Center, Cleveland, OH.

References

1. McKeown, S.A. and LeVasseur, R.D. High performance heat sink for surface mount applications, CH 3030-4/91/0000-0153, IEEE, 1991: 153-157.
2. Singh, M., Asthana, R., and Shpargel, T.P. Brazing of C-C composites to Cu-clad Mo for thermal management applications. Mater. Sci. Eng. A, 2007; 452-453: 699-704.
3. Taylor, R. Carbon Matrix Composites. In: Kelly A., Zweben, C., editors. Comprehensive Composite Materials, vol. 4: Carbon/Carbon, Cement and Ceramic Matrix Composites, Boston: Elsevier Science, 2000, 387-426.
4. Harper, C.A. Electronic Materials and Processes Handbook, New York: McGraw-Hill, 2003, 10.67-10.68.

5. Singh, M., Shpargel, T.P., Morscher, G.N., Asthana, R. Active metal brazing and characterization of brazed joints in titanium to carbon-carbon composites. Mater. Sci. Eng. A, 2005; 412-413: 123-128.
6. Morscher, G.N., Singh, M., Shpargel, T.P., Asthana, R. A simple test to determine the effectiveness of different braze compositions for joining Ti tubes to C/C composite plates. Mater. Sci. Eng. A, 2006; 418: 19-24.
7. Singh, M., Shpargel, T.P., Asthana, R. Brazing of stainless steels to yttria-stabilized-zirconia (YSZ) using Gold-base brazes for Solid oxide fuel cell applications. Int. J. Appl. Ceram. Tech., 2007; 4(2): 119-133.
8. Singh M., Asthana, R. Joining of advanced ultra-high-temperature ZrB_2-based ceramic composites using metallic glass interlayers. Mater. Sci. Eng. A, 2007; 460-461: 153-162.
9. Eustathopoulos, N., Nicholas, M.G., Drevet, B. Wettability at High Temperatures, Boston: Pergamon, 1999, 281-282.
10. Keene, B.J. Review of data of surface tension of pure metals. Int. Mater. Revs., 1993; 38: 157-192.
11. Standing, R., Nicholas, M. The wetting of alumina and vitreous carbon by copper-tin-titanium alloy. J. Mater. Sci., 1978; 13: 1509-1514.
12. Li, J.G. Kinetics of wetting and spreading of Cu-Ti alloys on alumina and glassy carbon substrates. J. Mater. Sci. Lett., 1992; 11: 1551-1554.
13. Grigorenko, N., Poluyanskaya, V., Eustathopoulos, N., Naidich, Y. In Interfacial Sci. of Ceram. Joining, Bellosi et al, editors, Boston: Kluwer, 1998, 69-78.
14. Sobczak, N., Sobczak, J., Ksiazek, M., Radziwill, W., Morgiel, J. In Proc. 2nd Int. Conf. on High-Temp. Capillarity, Eustathopoulos N., Sobczak, N., editors, Krakow: Foundry Research Institute, 1997, 97-98.
15. Sobczak, N., Sobczak, J., Rohatgi, P., Ksiazek, M., Radziwill W., Morgiel, J. In: Proc. Int. Conf. High-Temperature Capillarity, Krakow: Foundry Research Institute, Eustathopoulos, N., Sobczak, N., 1997, 145-151.
16. Park, J. -W., Mendez, P.F., Eagar, T.W. Strain energy distribution in ceramic-to-metal joints. Acta Mater., 2002; 50(5): 883-899.
17. Park, J. -W., Mendez, P.F., Eagar, T.W. Strain energy release in ceramic-to-metal joints by ductile metal interlayers. Scripta Mater., 2005; 53(7): 857-861.
18. Park, J. -W., Eagar, T.W. Strain energy relese in ceramic-to-metal joints with patterned intrelayers. Scripta Mater., 2004; 50(4): 555-559.
19. Kovalev, S.P., Miranzo, P., Osendi, M.I. J. Amer. Ceram. Soc., 1998; 81(9): 2342-2348.
20. Kimura, O. Effect of interlayer thickness of residual thermal stresses in a ceramic-to-metal cylinderical joint. J. Amer. Ceramc. Soc., 1993; 76: 757.
21. Yu, H.Y., Sanday, S.C., Rath, B.B. J. Amer. Ceram. Soc., 1993; 76: 1661.
22. http://www.composites-by-design.com/carbon-carbon.htm

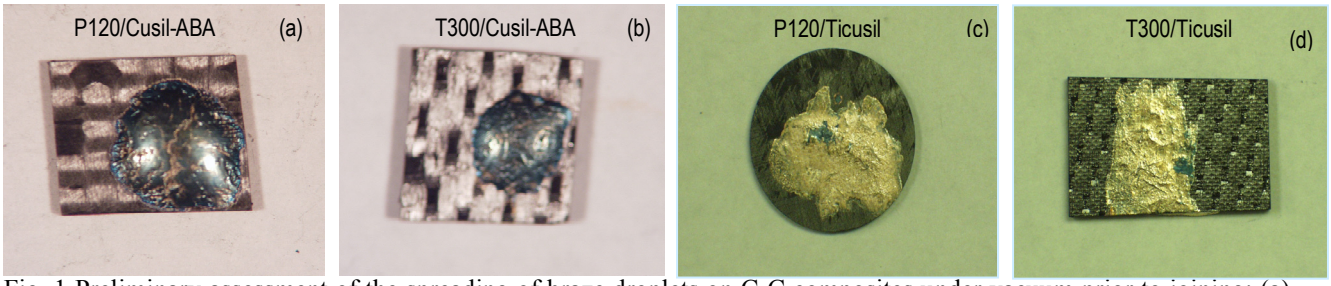

Fig. 1 Preliminary assessment of the spreading of braze droplets on C-C composites under vacuum prior to joining: (a) P120 C fiber-reinforced C-C composite/Cusil-ABA, (b) T300 C fiber-reinforced C-C composite/Cusil-ABA, (c) P120 C fiber-reinforced C-C composite/Ticusil, and (d) T300 C fiber-reinforced C-C composite/Ticusil.

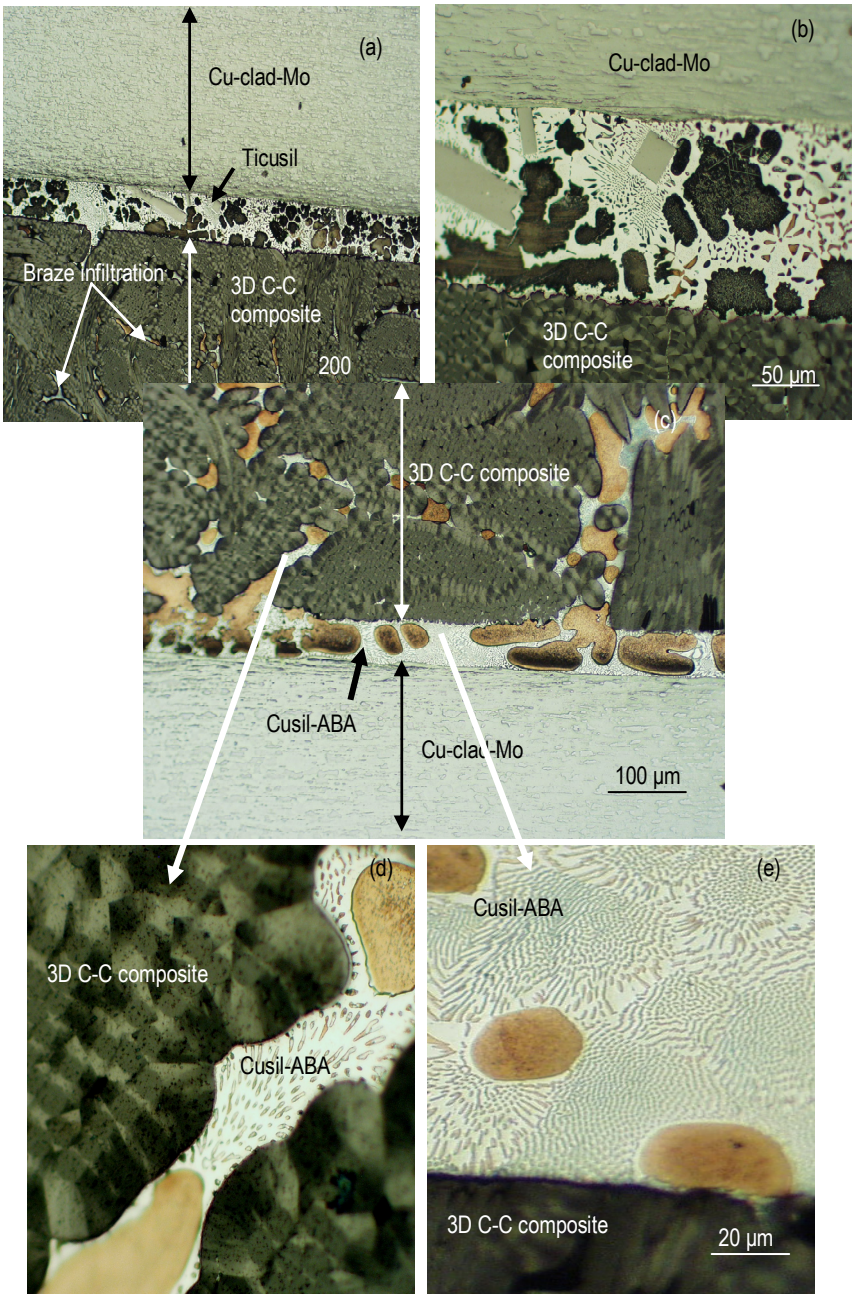

Fig. 2 Photomicrographs of a 3D C-C composite joined to Cu-clad-Mo using (a) & (b) Ticusil and (c)-(e) Cusil-ABA. Large-scale infiltration of inter-fiber channels by the molten brazes, and dissolution of Cu cladding in braze have occurred.

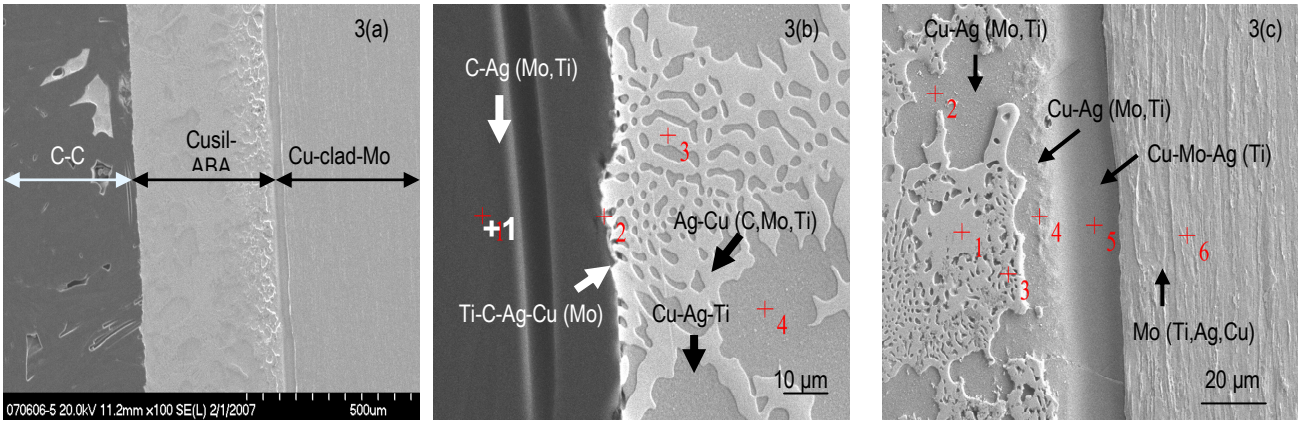

Fig. 3. A 3-D C-C (oriented fibers) composite/Cusil ABA/Cu-clad-Mo joint showing (a) overall view of the joint, (b) C-C/Cusil-ABA interface, and (c) Cusil-ABA/Cu-clad-Mo interface. The EDS analyses for points marked in (b) and (c) are given in Tables 2 and 3, respectively. Elements with a concentration less than ~3% are considered minor and shown in parentheses.

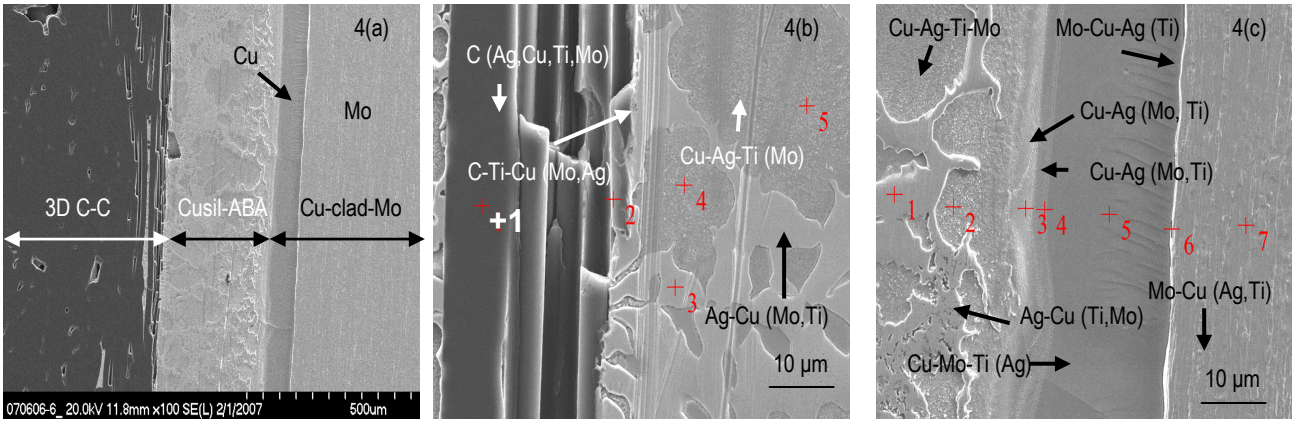

Fig. 4 A 3-D C-C (non-oriented fibers) composite/Cusil-ABA/Cu-clad-Mo joint showing (a) overall view of the joint, (b) C-C/Cusil-ABA interface, and (c) Cusil-ABA/Cu-clad-Mo interface. The EDS analyses for points marked in (b) and (c) are given in Tables 4 and 5, respectively.

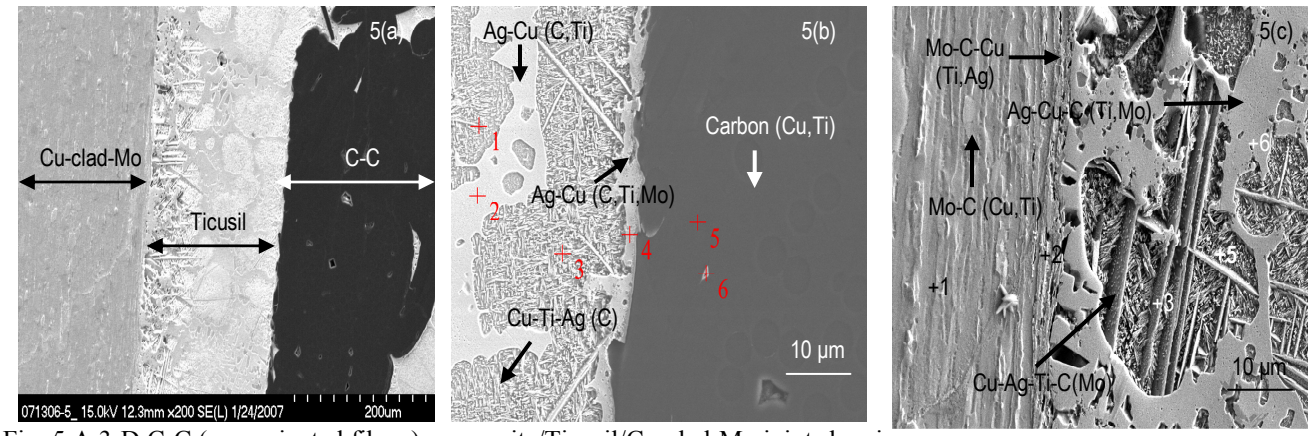

Fig. 5 A 3-D C-C (non-oriented fibers) composite/Ticusil/Cu-clad-Mo joint showir
C/Ticusil interface, and (c) Ticusil/Cu-clad-Mo interface. The EDS analyses for points marked in (b) and (c) are given in Tables 6 and 7, respectively.

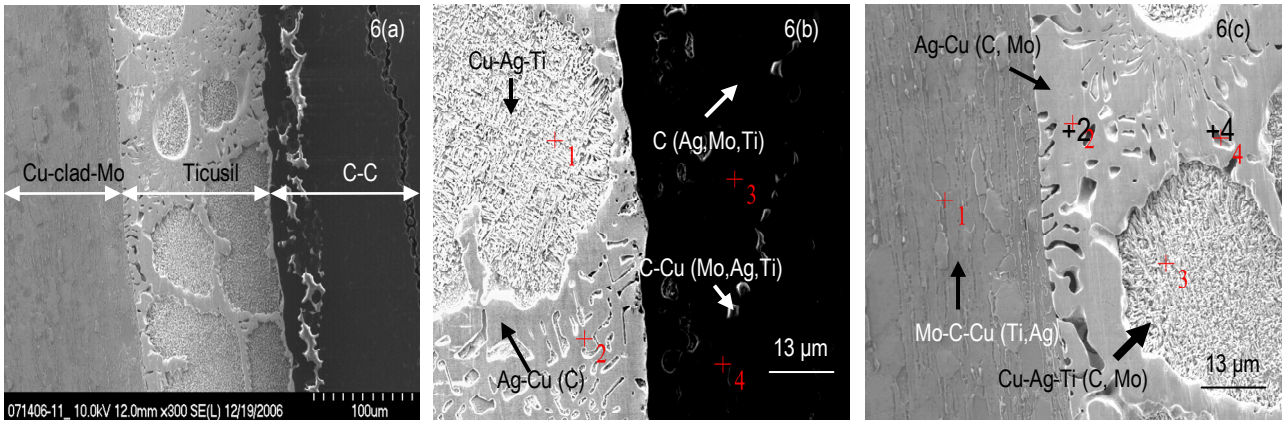

Fig. 6 A C-C (resin-derived) composite/Ticusil/Cu-clad-Mo joint showing (a) overall view of the joint, (b) C-C/Ticusil interface, and (c) Ticusil/Cu-clad-Mo interface. The EDS analyses for points marked in (b) and (c) are given in Tables 8 and 9, respectively.

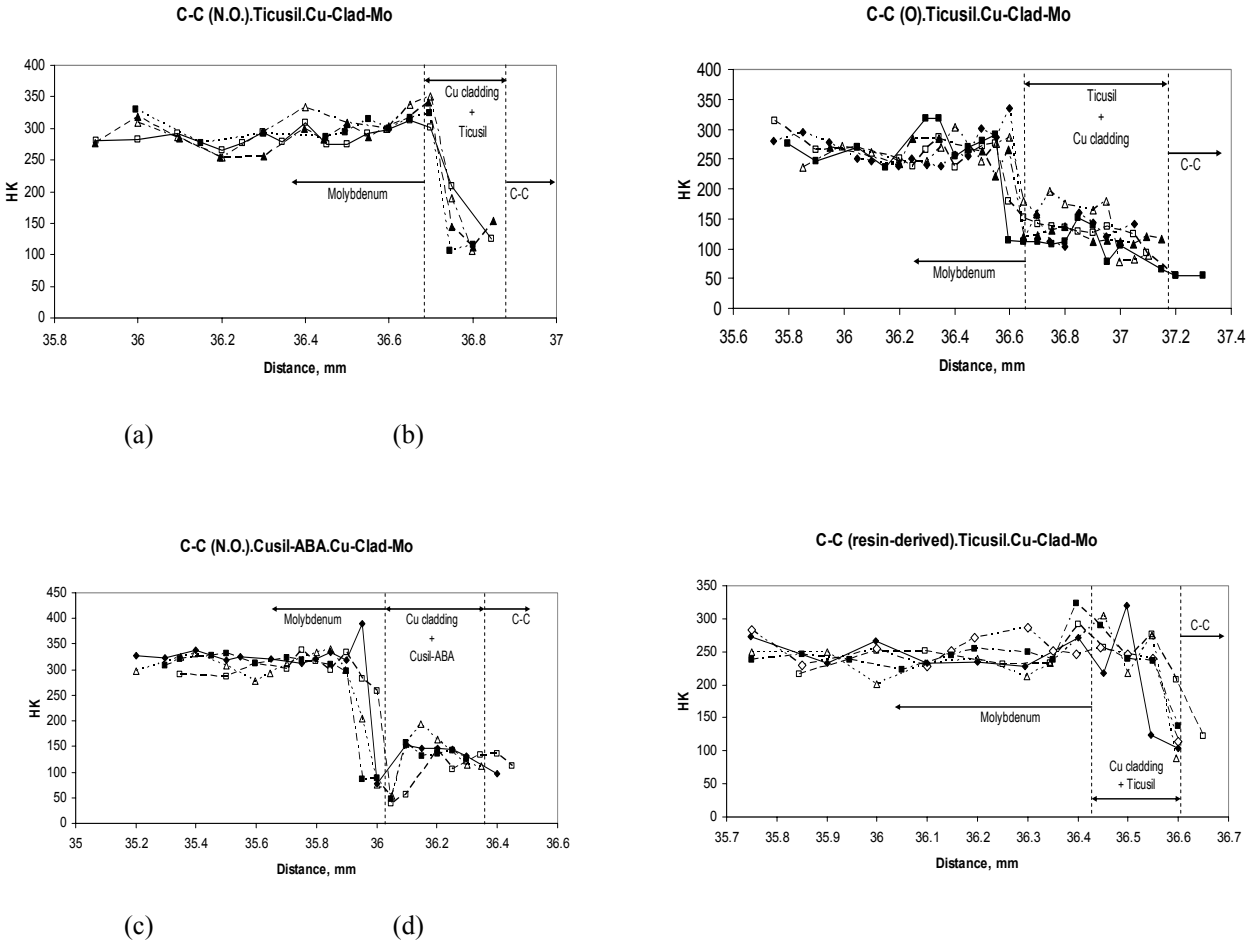

Fig. 7. Knoop hardness (HK) distribution across joints: (a) & (b) C-C/Ticusil/Cu-clad-Mo joint with (a) non-oriented C fibers at the mating surface and (b) oriented C fibers at the mating surface; (c) C-C/Cusil-ABA/Cu-clad-Mo joint with non-oriented fibers at the mating surface, and (d) resin-derived C-C composite/Ticusil/Cu-clad-Mo joint.

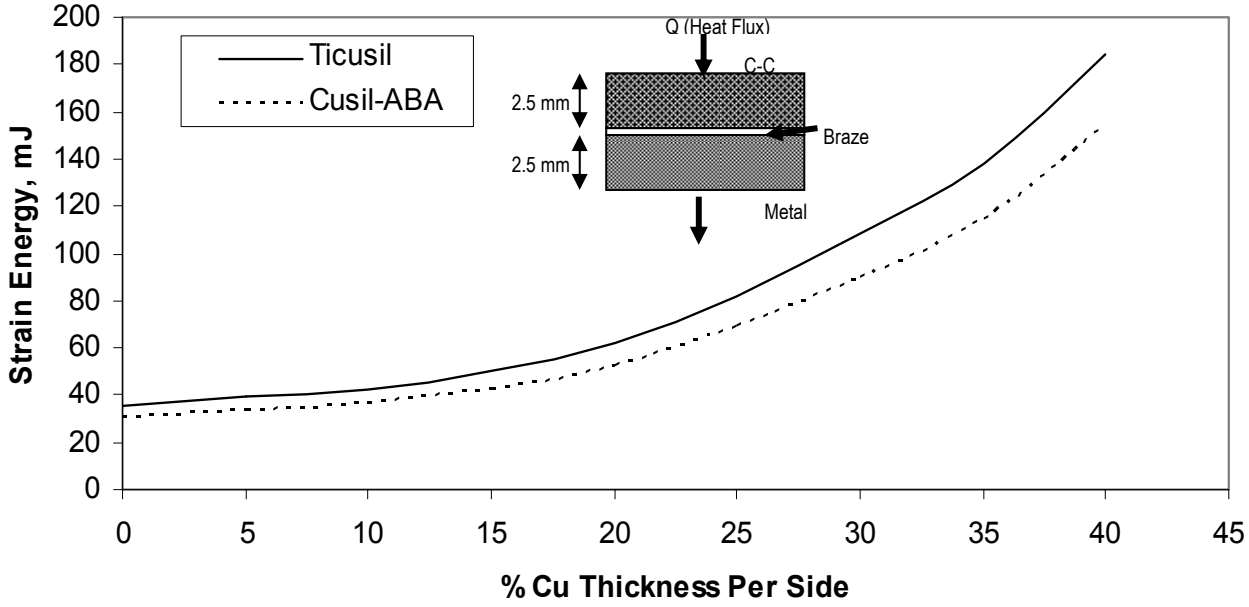
Ticusil
Cusil-ABA
Q (Heat Flux)
C-C
2.5 mm
Braze
2.5 mm
Metal
Strain Energy, mJ
% Cu Thickness Per Side
0
20
40
60
80
100
120
140
160
180
200
0
5
10
15
20
25
30
35
40
45

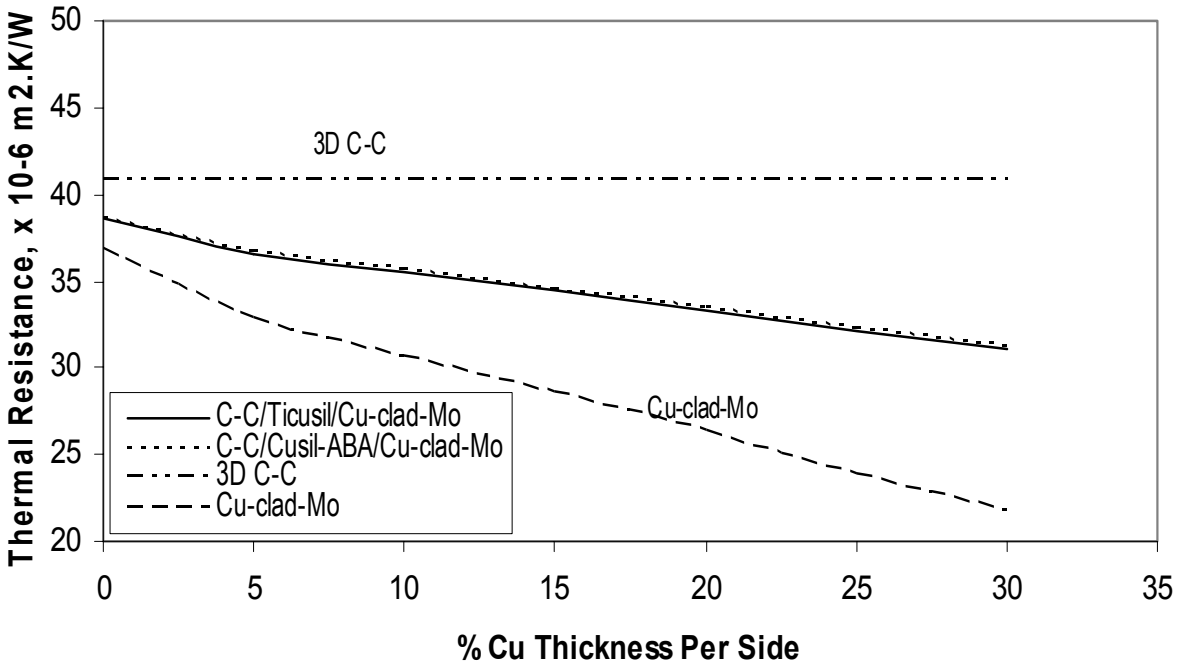

Fig. 8 Calculated (a) strain energy and (b) effective thermal resistance in the C-C/Cu-clad-Mo joint as a function of the % Cu thickness per side in Cu-clad-Mo.

Table 1. Composition and Selected Properties of Brazes used

Braze (composition, %)	**T_L, °C**	**T_S, °C**	**E, GPa**	**YS, MPa**	**UTS, MPa**	**CTE, $\times 10^{-6}$ C^{-1}**	**% El.**	**K, W/m.K**
Cusil-ABA® (63Ag-35.3Cu-1.75Ti)	815	780	83	271	346	18.5	42	180
Ticusil® (68.8Ag-26.7Cu-4.5Ti)	900	780	85	292	339	18.5	28	219

E: Young's modulus, YS: yield strength, UTS: tensile strength, CTE: coefficient of thermal expansion, %El: percent elongation, K: thermal conductivity. Cusil-ABA® and Ticusil® are active braze alloys from Morgan Advanced Ceramics, Hayward, CA.

Table 2. Relative Atomic Percentages of Elements in C-C composite/Cusil ABA/Cu-clad-Mo Joint of Fig. 3b

Location	C	Ti	Cu	Mo	Ag
Point 1	96.468	0.693	0.000	0.723	2.116
Point 2	35.131	49.912	5.203	0.941	8.813
Point 3	0.675	0.328	3.881	0.281	94.835
Point 4	0.000	2.437	89.469	0.000	8.094

Table 3. Relative Atomic Percentages of Elements in C-C composite/Cusil ABA/Cu-clad-Mo Joint of Fig. 3c

Location	Ti	Cu	Mo	Ag
Point 1	0.339	3.838	0.250	95.573
Point 2	0.801	87.267	1.159	10.773
Point 3	10.733	12.685	1.354	75.228
Point 4	1.346	86.443	1.361	10.850
Point 5	0.826	96.051	2.077	1.046
Point 6	1.155	0.515	97.672	0.658

Table 4. Relative Atomic Percentages of Elements in C-C composite/Cusil ABA/Cu-clad-Mo Joint of Fig. 4b

Location	C	Ti	Cu	Mo	Ag
Point 1	93.479	0.722	2.144	0.616	3.039
Point 2	85.396	9.160	3.100	0.805	1.538
Point 3	0.000	0.566	3.909	0.532	94.994
Point 4	0.000	4.161	87.138	0.261	8.441
Point 5	0.000	1.755	88.985	0.000	9.260

Table 5. Relative Atomic Percentages of Elements in C-C composite/Cusil ABA/Cu-clad-Mo Joint of Fig. 4c

Location	Ti	Cu	Mo	Ag
Point 1	1.000	4.661	0.275	94.063
Point 2	4.702	86.588	1.833	6.878
Point 3	1.557	94.313	1.937	2.192
Point 4	0.252	91.198	0.554	1.271
Point 5	1.312	96.747	1.790	0.151
Point 6	0.624	7.868	88.846	2.662
Point 7	0.439	1.177	97.438	0.946

Table 6. Relative Atomic Percentages of Elements in C-C composite/Ticusil/Cu-clad-Mo Joint of Fig. 5b

Location	C	Ti	Cu	Mo	Ag
Point 1	5.345	8.090	81.097	0.314	5.154
Point 2	2.097	0.228	4.540	0.508	92.627
Point 3	0.000	10.084	75.623	0.236	14.057
Point 4	1.852	0.368	3.776	0.382	93.623
Point 5	98.060	0.264	1.183	0.231	0.262
Point 6	26.237	54.484	16.697	0.553	2.030

Table 7. Relative Atomic Percentages of Elements in C-C composite/Ticusil/Cu-clad-Mo Joint of Fig. 5c

Location	C	Ti	Cu	Mo	Ag
Point 1	7.679	0.178	0.446	91.603	0.094
Point 2	14.986	0.227	4.036	80.515	0.235
Point 3	4.616	10.537	65.709	0.379	18.760
Point 4	5.039	42.850	50.659	0.398	1.054
Point 5	3.482	10.474	52.933	0.310	32.801
Point 6	2.330	0.167	1.981	0.212	95.310

Table 8. Relative Atomic Percentages of Elements in C-C composite/Ticusil/Cu-clad-Mo Joint of Fig. 6b

Location	C	Ti	Cu	Mo	Ag
Point 1	0.799	6.603	77.559	0.422	14.617
Point 2	2.198	0.495	9.874	0.460	86.973
Point 3	99.472	0.112	0.000	0.198	0.218
Point 4	78.303	0.527	18.766	1.136	1.268

Table 9. Relative Atomic Percentages of Elements in C-C composite/Ticusil/Cu-clad-Mo Joint of Fig. 6c

Location	C	Ti	Cu	Mo	Ag
Point 1	7.464	0.363	3.304	88.645	0.223
Point 2	1.171	0.264	8.930	0.498	89.138
Point 3	2.027	8.504	73.068	0.365	16.036
Point 4	0.000	0.058	6.198	0.657	93.087